# Measuring floating thick seep oil from the Coal Oil Point marine hydrocarbon seep field by quantitative thermal oil slick remote sensing

Ira Leifer[1], Christopher Melton[1], William Daniel[1], David M. Tratt[2], Patrick D. Johnson[2], Kerry N. Buckland[2], Jae Deok Kim[1], Charlotte Marston[1]

[1] Bubbleology Research International, Inc., Solvang, CA 93463
[2] The Aerospace Corporation, El Segundo, CA 90245

## S1. Brightness Temperature

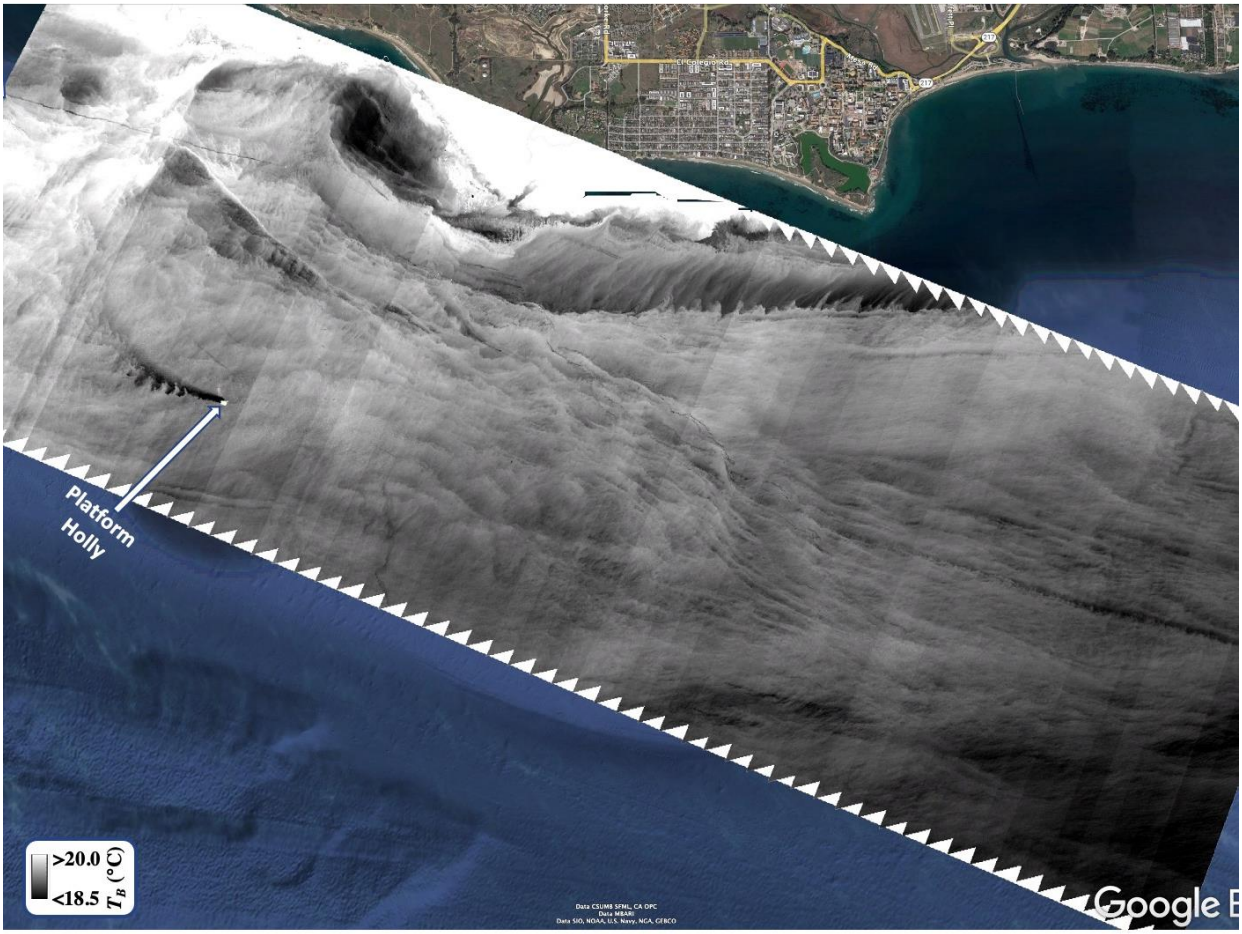


**Figure S1.** Brightness temperature, $T_B$, map of the COP seep field. Imagery acquired 29 August 2013, Platform Holly labeled. Data key on figure.

A wide range of thermal structures are evident in the brightness temperature map of the COP seep field and surrounding waters (**Figure S1**). Platform Holly is evident as a turbulent cool flow tracking the current in a wide arc that follows the inner downstream eddy to the west of Coal Oil Point (COP). The current shear off Isla Vista is associated with upwelling and colder water, as is the downstream eddy. The eddy combines with the along-shore current west of COP to move warmer offshore water eastwards towards the COP. Seeps upwell cold water [1], evident as a wake-like structures stretching downcurrent. This upwelling likely induces some convective-like structures to the southeast of COP, associated with the stronger La Goleta Seep and Trilogy Seep areas (also see **Figure 4A**).

## S2. Winds

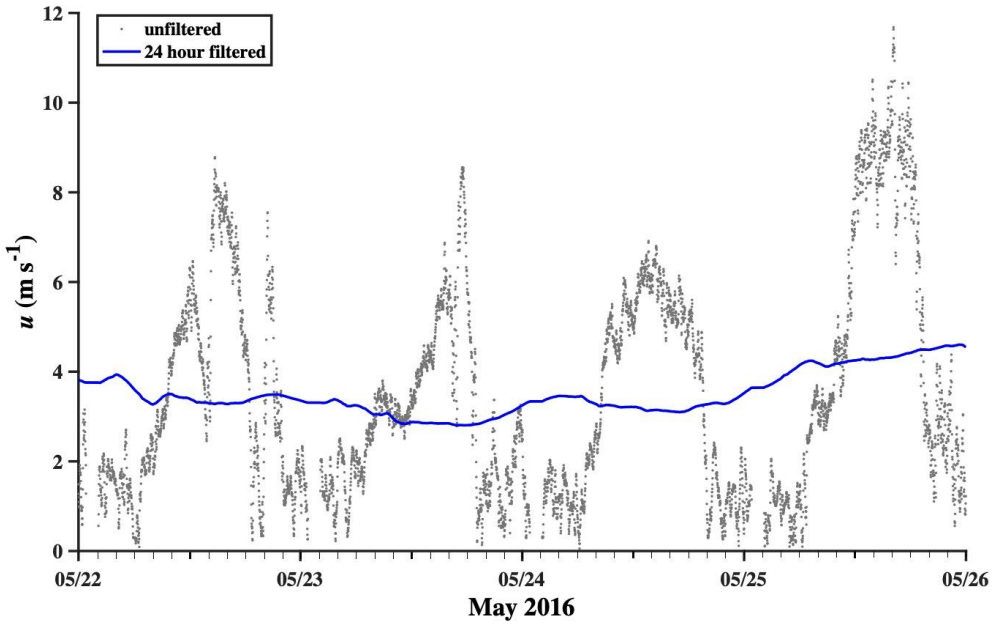


**Figure S2.** Unfiltered and 24-hr filtered winds at West Campus Station (WCS location in **Figure 4**) during the field experiment. Data key on the figure.

Winds showed strong diurnal patterns of elevated strength in the afternoon through early evening, collapsing to calm levels close to midnight (**Figure S2**). Winds also gradually strengthened from 22 May to 26 May 2016.

## S2. Currents

Hourly current data for 23 May and 25 May 2016 were downloaded from https://hfrnet-tds.ucsd.edu/thredds/HFRADAR_USWC.html, and were gap filled with the nearest neighbor in time and space and then nearest-neighbor smoothed (**Figure S3**). The CODAR data clearly show the current tidal ellipse. Early morning currents were stronger than late morning currents, albeit in a similar direction. The main difference between the 23 and 25 of May was that late evening currents were much stronger on the 25$^{th}$ than on the 23$^{rd}$. Also, evening currents on the 25$^{th}$ swung more sharply to offshore ~1800 LT (after field efforts were finished). Typical current speeds for around COP are 23±14 cm s$^{-1}$ for May 2016, calculated for a 5x5 grid of CODAR data.

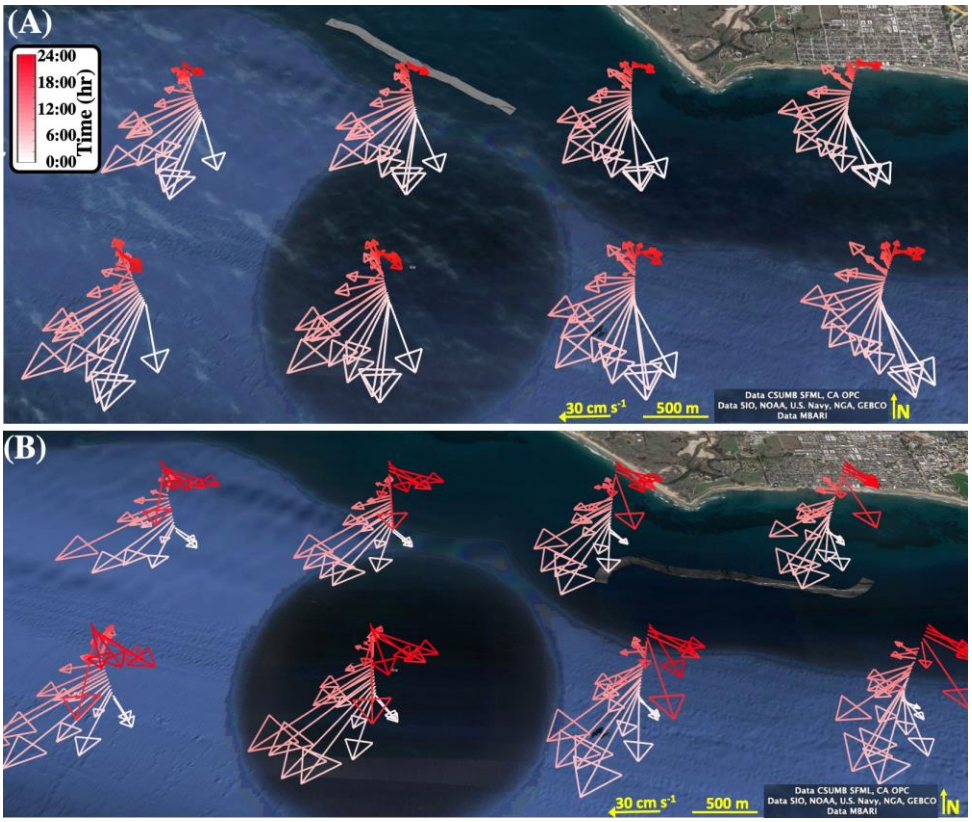


**Figure S3.** Hourly current radar (CODAR) for (**A)** 23 May 2016 and (**B)** 25 May 2016. Data key on figure. SeaSpires thermal infrared slick mosaic on each day shown. Shown in the Google Earth environment.

## S3. Sea surface water and oil temperatures

*S3.1. Brightness Temperature Contrast: Collects*

$\Delta T_{BO}$ is relative to the water brightness temperature ($T_{BW}$). For the collects, $T_{BW}$ is derived from the scene's $T_B$ probability distributions, $\Phi(T_B)$, which were analyzed to identify the different scene elements (**Figure S4**). Specifically, the oil temperature probability distribution was modeled by a broad distribution, $\Phi_O$, and two narrower distributions modeled the oil-free water, $\Phi_W$, and the wake, $\Phi_{W1}$,

$$\Phi = \Phi_o + \Phi_W + \Phi_{W1} = a_{\mathrm{o}}\, e^{-\frac{(T_{BP\_O}-T_B)^2}{\sigma_{\mathrm{O}}^2}} + a_{\mathrm{W}} e^{-\frac{(T_{BP\_W}-T_B)^2}{\sigma_{\mathrm{W}}^2}} + a_{\mathrm{W1}} e^{-\frac{(T_{BP\_W1}-T_B)^2}{\sigma_{\mathrm{W1}}^2}} \qquad \text{(S1)}$$

where $a_o$, $a_W$, and $a_{W1}$ are the amplitudes or maxima of the distributions, $\Phi_O$, $\Phi_W$, and $\Phi_{W1}$, for the oil, water, and wake masses, respectively, with distribution half-widths, $\sigma_O$, $\sigma_W$, and $\sigma_{W1}$ and peaks at $T_{BP\_o}$, $T_{BP\_W}$, and $T_{BP\_W1}$. $\Phi_O$ is significantly broader than for water, $\Phi_W$, which is expected given that oil thickness, $h$, spans orders of magnitude and the functional dependency of $h(\Delta T_B)$. In **Figure S4**, $\Phi_O$ is cooler than the water Gaussian functions, $\Phi_W$ and $\Phi_{W1}$, 13.1°C for oil versus 13.5°C and 13.75°C for the wake and seawater. Thus, in this case, $T_B$ for oil is less than for water because $\varepsilon$ is lower for oil than for seawater.

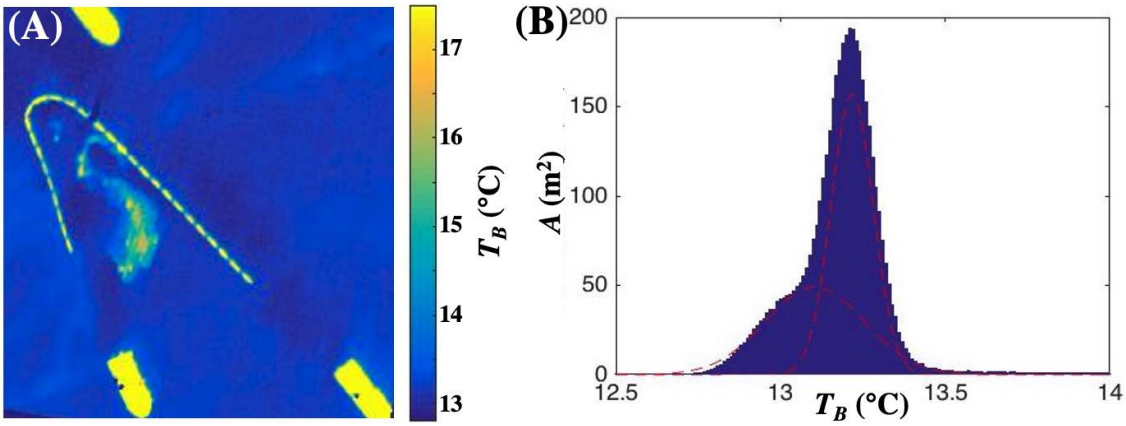


**Figure S4.** (**A)** Thermal infrared image of a "Collect." (**B)** Sea surface area, $A$, versus $T_B$ for the image in panel A. Also shown are Gaussian fits to water and oil. Data key on the figure.

### S3.2. Brightness Temperature Contrast: Slick Surveys

Prior to modeling the sea surface cross-slick $T_B$ profile, outliers were removed in the cross-slick temperature profile, $T_{BW}(Y)$. Water pixels were identified as those for which $T_B$ lies within the range where $\Phi_W > 0.01a_W$ are classified as water. Outliers were defined based on $\sigma$ derived from $\Phi_W(T_B)$ from **Eqn. S1**. Where there were two water masses on either side of the slick, $\Phi$ was modeled by two Gaussian functions and $\sigma = (\sigma_W + \sigma_{W1})/2$ (**Figure S5B**). A 1-m moving average of $T_{BW}(Y)$ was used to identify further outliers. Specifically, outliers are defined as more than $2\sigma$ from the moving average and are interpolated.

$T_{BW}(Y)$ is determined from a combination of a linear polynomial and a sinusoidal function fit to non-outlier water pixels, i.e.,

$$T_{Bw}(Y) = b + cY + \sin(dY), \tag{S2}$$

where $b$, $c$, and $d$ are fit parameters. $T_{BW}(Y)$ is a two-part piecewise linear function with a transition that gap fills from $y_1$ to $y_2$, i.e., across the oil slick location where there is a discontinuity. A Gaussian transition function gap-fills,

$$f(Y) = f_1(Y)\left(1 - e^{-\frac{(y_1-Y)^2}{(y_1-y_2)^2}}\right) + f_2(Y)e^{-\frac{(y_2-Y)^2}{(y_1-y_2)^2}} \tag{S3}$$

using two functions, $f_1$ and $f_2$. The transition function is smooth through the second derivative. Evaluation of $T_{BW}(Y)$ from $y_1$ to $y_2$ provides $T_{BW}(Y)$ for the oil slicks pixels, i.e., $T_{BW}$ if there was no oil. $T_{BW}(Y)$ is evaluated for each image strip centered at the along-slick location, $X$, *i.e.*, $T_{Bw}(X,Y)$. The brightness temperature contrast profile, $\Delta T_B(Y)$, relative to the water, is

$$\Delta T_B(X,Y) = T_B(X,Y) - T_{BW}(X,Y), \tag{S4}$$

for $y_1 < Y < y_2$. $\Delta T_B(X,Y)$ is calculated by assuming a linear trend with $X$ between image subsets. Given the narrow width of the image subsets (50 m, 250 pixels), errors from non-linearity are small. Additionally, adjacent image subsets have ~90% overlap. Overlapping $\Delta T_B(X,Y)$ values between adjacent image subsets are averaged.

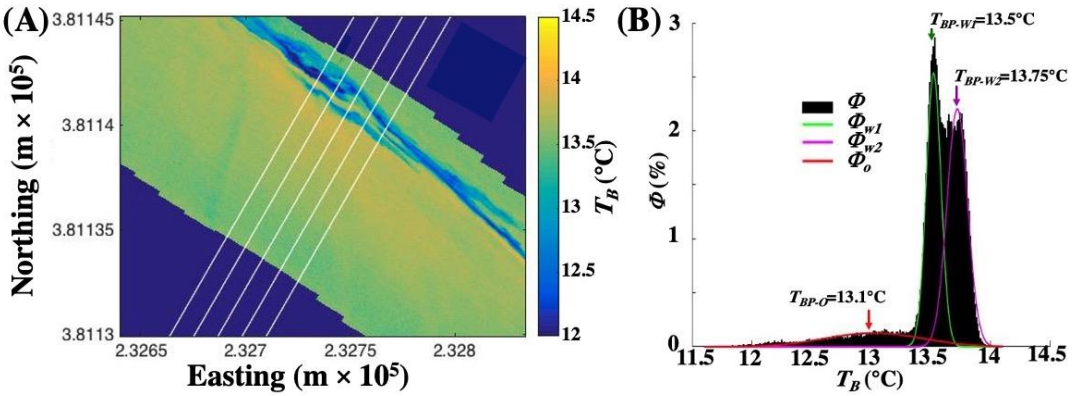


**Figure S5.** (**A)** Slicks survey image, (**B)** Sea surface $T_B$ probability distribution, $\Phi$, for the image in panel A. Also shown are Gaussian fits to water, $\Phi_{W1}$ and $\Phi_{W2}$, and oil, $\Phi_O$, and their respective peaks, $T_{BP\text{-}W1}$, $T_{BP\text{-}W2}$, $T_{BP\text{-}O}$. Data key on the figure. Acquired 23 May.

## S4. Uncertainty

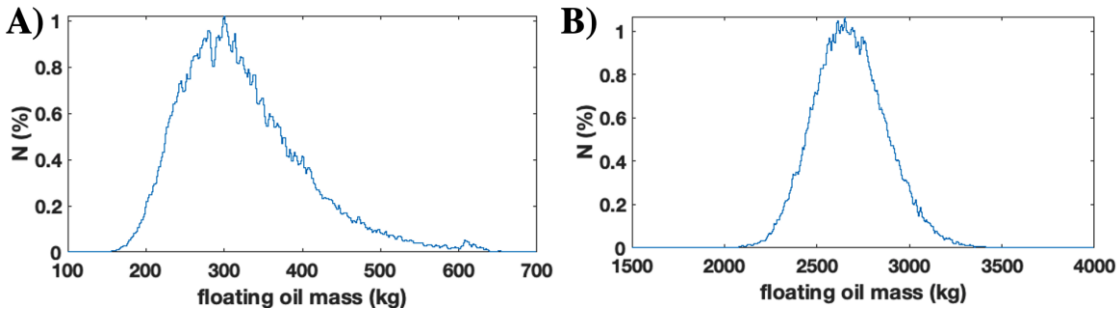


**Figure S6.** Monte Carlo simulation probability distribution function, $N$, for **A)** 23 May and **B)** 25 May.

## References

1. Leifer I, Jeuthe H, Gjøsund SH, Johansen V. 2009. Engineered and natural marine seep, bubble-driven buoyancy flows. *Journal of Physical Oceanography* **39**(12): 3071-3090. doi:10.1175/2009JPO4135.1.

## Table of Nomenclature and Symbols

| | | |
|---|---|---|
| CODAR | - | Coastal Ocean Dynamics Application Radar |
| COP | | Coal Oil Point |
| $a_o$ | (-) | amplitude of $\Phi_o(T_B)$ |
| $a_W$ | (-) | amplitude of $\Phi_W(T_B)$ |
| $a_{W1}$ | (-) | amplitude of $\Phi_{W1}(T_B)$ |
| $b$ | (°C) | Sea surface profile temperature fit parameter |
| $c$ | (°C m$^{-1}$) | Sea surface profile temperature fit parameter |
| $d$ | rad m$^{-1}$ | Sea surface profile temperature fit parameter |
| $E$ | kg day$^{-1}$ | Oil emissions |
| $f(y)$ | m | Generalized gap-filling function |
| $h$ | cm | Oil slick thickness |
| $h_T$ | cm | Critical oil slick thickness |
| $k$ | - | Scaling parameter |
| $M$ | kg | Collected oil mass |
| $N$ | (-) | Monte Carlo simulation probability distribution |
| $T_{BP-o}$ | (°C) | Peak temperature of fit to $\Phi_o(T_B)$ |
| $T_{BP-W}$ | (°C) | Peak temperature of fit to $\Phi_W(T_B)$ |

| | | |
|---|---|---|
| $T_{BP-W1}$ | (°C) | Peak temperature of fit to $\Phi_{W1}(T_B)$ |
| $T$ | °C | Temperature |
| $T_B$ | °C | Brightness temperature |
| $T_{BO}$ | °C | Oil brightness temperature |
| $T_{BW}$ | °C | Water brightness temperature |
| $T_{BW}(y)$ | °C | Cross slick $T_B$ profile |
| $T_o$ | °C | Interfacial oil Temperature |
| $T_W$ | °C | Water temperature |
| $x$ | m | Along slick coordinate |
| $y$ | m | Cross slick coordinate |
| $y_1$ | m | Parameter from generalized gap-filling function |
| $y_2$ | m | Parameter from generalized gap-filling function |
| $\Delta T_{Bo}$ | °C | Oil brightness temperature contrast |
| $\Phi$ | - | Pixel $T_B$ probability distribution |
| $\Phi_O$ | - | Oil $T_B$ probability distribution |
| $\Phi_W$ | - | Seawater $T_B$ probability distribution |
| $\Phi_{W1}$ | - | Wake water $T_B$ probability distribution |
| $\varepsilon$ | - | Emissivity |
| $\varepsilon_O$ | - | Oil emissivity |
| $\varepsilon_W$ | - | Water emissivity |
| $\sigma$ | | Standard deviation |
| $\sigma_o$ | | Half-width of fit to $\Phi_O$ |
| $\sigma_W$ | | Half-width of fit to $\Phi_W$ |
| $\sigma_{W1}$ | | Half-width of fit to $\Phi_{W1}$ |